

See discussions, stats, and author profiles for this publication at: <https://www.researchgate.net/publication/5671800>

The intrastriatal injection of thrombin in rat induced a retrograde apoptotic degeneration of nigral dopaminergic neurons through synaptic elimination

ARTICLE *in* JOURNAL OF NEUROCHEMISTRY · JUNE 2008

Impact Factor: 4.28 · DOI: 10.1111/j.1471-4159.2007.05170.x · Source: PubMed

CITATIONS

9

READS

5

8 AUTHORS, INCLUDING:



[Jose L Venero](#)

Universidad de Sevilla

101 PUBLICATIONS 2,930 CITATIONS

SEE PROFILE

The intrastriatal injection of thrombin in rat induced a retrograde apoptotic degeneration of nigral dopaminergic neurons through synaptic elimination

Antonio J. Herrera, Rocío M. de Pablos, Eloisa Carreño-Müller, Ruth F. Villarán, José L. Venero, Mayka Tomás-Camardiel, Josefina Cano and Alberto Machado

Departamento de Bioquímica, Bromatología, Toxicología y Medicina Legal, Facultad de Farmacia, Universidad de Sevilla, Sevilla, Spain

Abstract

We have performed intrastriatal injection of thrombin and searched for distant effects in the cell body region. In striatum, thrombin produced a slight loss of striatal neurons as demonstrated by neural nuclei immunostaining – a non-specific neuronal marker – and the expression of glutamic acid decarboxylase 67 mRNA, a specific marker for striatal GABAergic interneurons, the most abundant phenotype in this brain area. Interestingly, striatal neuropil contained many boutons immunostained for synaptic vesicle protein 2 and synaptophysin which colocalize with tyrosine hydroxylase (TH), suggesting a degenerative process with pre-synaptic accumulation of synaptic vesicles. When we studied the effects on substantia nigra, we found the disappearance of dopaminergic neurons, shown by loss of TH immunoreactivity,

loss of expression of TH and dopamine transporter mRNAs, and disappearance of FluoroGold-labelled nigral neurons. The degeneration of substantia nigra dopaminergic neurons was produced through up-regulation of cFos mRNA, apoptosis and accumulation of α -synuclein shown by colocalization experiments. Thrombin effects could be mediated by protease-activated receptor 4 activation, as protease-activated receptor 4-activating peptide mimicked thrombin effects. Our results point out the possible relationship between synapse elimination and retrograde degeneration in the nigral dopaminergic system.

Keywords: haemorrhage, neuronal death, Parkinson's disease, retrograde, striatum, substantia nigra.

J. Neurochem. (2008) **105**, 750–762.

Parkinson's disease (PD) is characterized by the progressive degeneration of the substantia nigra (SN) dopaminergic neurons, leading to loss of more than 80% of dopamine (DA) and the manifestation of clinical symptoms. Most cases of PD are non-familial and sporadic with undefined cause, although different forms of familial PD have been mapped to particular chromosomal regions; so, alterations in the gene for α -synuclein (α -syn) were identified in one inherited form (Kruger *et al.* 1998; Farrer *et al.* 1999; Chartier-Harlin *et al.* 2004). A currently yet unconfirmed concept is that degenerative processes may start at the nerve terminals of dopaminergic neurons (Sauer and Oertel 1994). In adult animals, this could result from energy impairment at their terminal projection site (Sonsalla *et al.* 1997). During development, retrograde degeneration of dopaminergic neurons in substantia nigra pars compacta (SNc) occurs through an apoptotic process (Burke *et al.* 1992; Macaya *et al.* 1994); this event was justified by the loss of target-derived

retrogradely transported trophic factors, according to classic concepts.

In a previous work, we described the specific degeneration of dopaminergic neurons in SN after the injection of

Received July 25, 2007; revised manuscript received September 14, 2007; accepted November 27, 2007.

Address correspondence and reprint requests to Dr Alberto Machado, Departamento de Bioquímica, Bromatología, Toxicología y Medicina Legal, Facultad de Farmacia, Universidad de Sevilla, c/ Profesor García González, 2, Sevilla 41012, Spain. E-mail: machado@us.es

Abbreviations used: α -syn, α -synuclein; BSA, bovine serum albumin; DA, dopamine; DAT, dopamine transporter; FG, FluoroGold; GAD, glutamic acid decarboxylase; GFAP, glial fibrillary acidic protein; ICH, intracerebral haemorrhage; NeuN, neural nuclei; PAR, protease-activated receptor; PBS, phosphate-buffered saline; PBT, Triton X-100 in PBS; PD, Parkinson's disease; SN, substantia nigra; SNc, substantia nigra pars compacta; SSC, standard saline citrate; SV2, synaptic vesicle protein 2; SYP, synaptophysin; TBS, Tris-buffered saline; TdT, terminal transferase; TH, tyrosine hydroxylase; TH-IR, tyrosine hydroxylase immunoreactivity; TUNEL, terminal uridine nick-end labelling.

thrombin (Carreño-Müller *et al.* 2003). This effect has been confirmed by others (Choi *et al.* 2003a, Choi *et al.* 2003b). Contrary to the clear-cut effect observed in SN, injection of thrombin within the striatum produced a reduced inflammatory reaction without apparent effect on either dopaminergic terminals or neuronal bodies except for the appearance of encapsulated oedematous structures. However, when we have carried out a more careful and longer study on the effect of thrombin injection within the striatum [where tyrosine hydroxylase immunoreactivity (TH-IR) displayed a normal pattern], we have found loss of TH-IR in the SN and of fibres connecting this structure with the striatum. This could be an important finding, since this is the first time that a retrograde loss of the dopaminergic system is described in adult animals without a significant striatal degeneration or inhibition of the energy-producing metabolism.

Thrombin activates several members of the protease-activated receptor (PAR) family that are widely distributed throughout the CNS. Thrombin cleaves amino terminal exodomain of PAR1, -3 and -4; the newly generated amino terminus binds to the extracellular domain of the receptor as a tethered ligand (Noorbakhsh *et al.* 2003). All PARs (PAR1–4) are widely expressed in the rodent brain (Weinstein *et al.* 1995; Striggow *et al.* 2001). Receptor activation triggers intracellular signal transduction pathways, including increase in intracellular calcium (Smith-Swintosky *et al.* 1995), decrease in cAMP (Yang *et al.* 1997) and activation of protein kinase C (Wang *et al.* 2002). Thrombin induces morphological alterations in neurons and glial cells (Beecher *et al.* 1994) and has the ability to eliminate synapses (Zoubine *et al.* 1996); thus, it has been speculated that this protease regulates growth and differentiation processes within the CNS. Therefore, in the present study we aimed to examine the retrograde degenerative changes in the SN and in some fibres connecting this structure with the striatum following an intrastriatal injection of thrombin. We propose that thrombin is able to induce a retrograde degeneration of the dopaminergic system from striatum, possibly through the activation of PAR4 along with the destruction of pre-synaptic elements with the consequent synapse elimination.

Materials and methods

Animals and surgery

Female albino Wistar rats (200–300 g) were used for these studies. Animals were kept at constant room temperature of $22 \pm 1^\circ\text{C}$ and relative humidity (60%) with a 12-h light–dark cycle with free access to food and water. Rats were anaesthetized with chloral hydrate (400 mg/kg) and positioned in a stereotaxic apparatus (Kopf Instruments, Tujunga, CA, USA) to conform to the brain atlas of Paxinos and Watson (1986). Injections into the striatum were made 0.5 mm anterior, 3.0 mm lateral and 6.4 mm ventral to the bregma.

Animals were injected into the left striatum either 15 or 25 U of thrombin (from bovine plasma; thrombin lyophilized powder, 40–300 NIH U/mg protein from Sigma, St Louis, MO, USA) dissolved in 1% Monastral Blue inert tracer in saline solution in a final volume of 2 μL ; control animals received heat-denatured thrombin in an amount equivalent to 25 U of thrombin. The injections were delivered over a period of about 5 min; the needle was left *in situ* for another 10 min to avoid reflux along the injection track. For the PAR experiments, animals received 100 μg of the corresponding PAR1 (SFFLRN) and PAR4 (GYPGKF) activating peptides. At least five animals were used for each group.

Experiments were carried out in accordance with the Guidelines of the European Union Council (86/609/EU), following the Spanish regulations (BOE 67/8509-12, 1988) for the use of laboratory animals and approved by the Scientific Committee of the University of Sevilla, Sevilla, Spain.

Immunohistological evaluation: glial fibrillary acidic protein, OX-6, neural nuclei and tyrosine hydroxylase

Rats were perfused through the heart under deep anaesthesia (chloral hydrate) with 150–200 mL of 4% *p*-formaldehyde in phosphate buffer, pH 7.4. Brains were removed and then cryoprotected serially in sucrose in phosphate-buffered saline (PBS), pH 7.4, first in 10% sucrose for 24 h and then in 30% sucrose until sunk (2–5 days). Brains were then frozen in isopentane at -15°C , and 25- μm sections were cut on a cryostat and mounted in gelatin-coated slides. Primary antibodies used were mouse-derived anti-glial fibrillary acidic protein (anti-GFAP, 1 : 300; Chemicon International Inc., Temecula, CA, USA), mouse-derived OX-6 (1 : 200; Serotec, Oxford, UK), mouse-derived anti-neuronal nuclei (anti-NeuN, 1 : 1000; Chemicon International Inc.) and mouse-derived anti-tyrosine hydroxylase (TH, 1 : 1000; Chemicon International Inc.). Sections were washed and then treated with 0.3% H_2O_2 in methanol for 30 min, washed again and incubated in a solution containing Tris-buffered saline (TBS) and 1% horse serum for 60 min in a humid chamber. Slides were drained and further incubated with the primary antibody in TBS containing 1% horse serum and 0.25% Triton X-100 for 24 h. Sections were then incubated for 2 h with biotinylated horse anti-mouse IgG (1 : 200; Vector Laboratories Inc., Burlingame, CA, USA) followed by a second 1-h incubation with ImmunoPure® ABC Peroxidase staining kit (Pierce, Rockford, IL, USA). The antibody was diluted in TBS containing 0.25% Triton X-100, and its addition was preceded by three 10-min rinses in TBS. The peroxidase was visualized with a standard diaminobenzidine/hydrogen reaction for 5 min.

Histochemistry data analysis

An ANALYSIS® image software (Soft Imaging System GmbH, Münster, Germany) couple to a Polaroid DMC camera (Polaroid, Cambridge, MA, USA) attached to a Leika light microscope (Leika Mikroskopie, Wetzlar, Germany) was used for the measures of the areas lacking NeuN immunostaining. The GFAP-positive population was evaluated by counting the number of cells per section. In each section, a systematic sampling of the area occupied by the GFAP-positive cells was made from a random starting point with a grid adjusted to count five fields per section. An unbiased counting frame of known area ($40 \times 25 \mu\text{m} = 1000 \mu\text{m}^2$) was superimposed on the tissue section image under a 100 \times oil immersion objective. The

number of neurons in the SN was estimated using a fractionator sampling design (Gundersen *et al.* 1988). Counts were made at regular predetermined intervals ($x = 150 \mu\text{m}$ and $y = 200 \mu\text{m}$) within each section. A systematic sample of the area occupied by the SN was made from a random starting point. An unbiased counting frame of known area ($40 \times 25 \mu\text{m} = 1000 \mu\text{m}^2$) was superimposed on the tissue section image under a $100\times$ oil immersion objective. Therefore, the area sampling fraction is $1000/(150 \times 200) = 0.033$. The entire z -dimension of each section was sampled; hence, the section thickness sampling fraction was 1. In all animals, $30\text{-}\mu\text{m}$ sections, each $150 \mu\text{m}$ apart, were analysed; thus, the fraction of sections sampled was $30/150 = 0.20$. The total number of neurons in the SN was estimated by multiplying the number of neurons counted within the sample regions by the reciprocals of the area sampling fraction and the fraction of section sampled.

Preparation of riboprobes

The rat TH cDNA cloned in PGEM-4Z as a 380-bp *EcoRI*–*KpnI* insert was kindly provided by Dr P. Sokoloff (INSERM, Paris, France). To prepare the TH antisense riboprobe this plasmid was linearized with *EcoRI* and used as a template with the T7 RNA polymerase (Erlander *et al.* 1991). To prepare the TH sense riboprobe plasmid was linearized with *SmaI* and used as a template with the Sp6 RNA polymerase (Erlander *et al.* 1991).

The rat dopamine transporter (DAT) cDNA contained in an 800-bp *XbaI*–*HindIII* fragment cloned in pRc/CMV (Invitrogen Corporation, Carlsbad, CA, USA) was kindly provided by Dr M. P. Martres (INSERM). This plasmid was linearized with *XbaI* and used as a template with the T7 RNA polymerase to prepare the DAT antisense riboprobe. To prepare the DAT sense riboprobe the same plasmid was linearized with *HindIII* and used as a template with the Sp6 RNA polymerase (Erlander *et al.* 1991).

pBluescript SK plasmids, containing the cDNA sequence for glutamic acid decarboxylase 67 (GAD67) as a 3.2-kb *EcoRI* insert (clones 14 and 18), were kindly provided by Dr A. Tobin (UCLA, Los Angeles, CA, USA). The GAD67 cDNA was isolated from a 1 gt-11 cDNA library made from poly(A) RNA from adult rat brain (Erlander *et al.* 1991). To prepare the GAD67 antisense transcript, clone 14 was digested with *SaI* and used as a template with the T3 RNA polymerase. To prepare the GAD67 sense transcript, clone 18 was digested with *SaI* and used as a template with the T3 RNA polymerase.

The PGEM-4Z plasmid containing the cDNA sequence for rat cFos was kindly provided by Dr P. Sokoloff (INSERM). The fragment corresponds to nucleotides 588–795 of rat cFos. To prepare the cFos antisense riboprobe, this plasmid was linearized by *EcoRI* and used as a template with the T7 RNA polymerase.

Sense and antisense riboprobes used for *in situ* hybridization were transcribed in the presence of [^{35}S]UTP (1300 Ci/mmol; Amersham International, Little Chalfont, UK). Single-strand antisense cRNA probes were synthesized with RNA polymerases according to a protocol provided by the RNA polymerase supplier (Bethesda Research Laboratories, Bethesda, MD, USA).

Isotopic *in situ* hybridization histochemistry

In situ hybridization on brain frozen sections was carried out as described in detail elsewhere (Carreño-Müller *et al.* 2003). Animals for cFos mRNA hybridization were decapitated at different times

after thrombin injection (6, 12, 24, 48 and 72 h), while animals for TH, DAT and GAD mRNAs were decapitated 1 week after thrombin injection. Thaw-mounted $12\text{-}\mu\text{m}$ sections were post-fixed for 30 min in 4% *p*-formaldehyde, followed by three 10 min washes in PBS (pH 7.4). Sections were treated for 1 min in 0.1 mol/L triethanolamine, followed by 10 min in acetic anhydride/0.1 mol/L triethanolamine in order to decrease non-specific binding. Following a 1 min wash in $2\times$ standard saline citrate (SSC), sections were dehydrated in a series of increasing concentrations of ethanol and then air-dried. The sections were hybridized for 3 h at 50°C with the [^{35}S] cRNA, rinsed in $4\times$ SSC/20 mmol/L dithiothreitol, then $4\times$ SSC alone. Sections were subjected to 30 min of RNase digestion at 37°C (20 $\mu\text{g/mL}$ RNase A in 0.5 mol/L NaCl, 0.01 mol/L Tris–HCl and 0.001 mol/L EDTA, pH 8.0), washed for 2 h in $2\times$ SSC at 25°C followed by $0.1\times$ SSC at 60°C for 1 h, dehydrated in a series of ethanol, air-dried, and processed for emulsion autoradiography. Autoradiograms were generated by apposing the labelled tissue to β max Hyperfilm (Eastman Kodak, Rochester, NY, USA) for 2 weeks.

In situ hybridization data analysis

The TH- and DAT-positive population was evaluated by counting the number of cells per section. In each section, a systematic sampling of the area occupied by the TH- and DAT-positive cells was made from a random starting point with a grid adjusted to count five fields per section. An unbiased counting frame of known area ($40 \times 25 \mu\text{m} = 1000 \mu\text{m}^2$) was superimposed on the tissue section image under a $100\times$ oil immersion objective.

Immunofluorescence

Animals were perfused and sections were prepared as described above. For immunofluorescence of synaptic vesicle protein 2 (SV2) and double-labelling of TH with synaptophysin (SYP), PAR4 and α -syn, sections were rehydrated in PBS for 10 min, and then blocked with PBS containing 1% normal horse serum for 1 h. The blocking solution was replaced for anti-TH (1 : 1000) or anti-SV2 (1 : 100) diluted in the blocking solution containing 0.25% Triton X-100, and the slides were then incubated overnight at 4°C . The slides were washed three times in PBS and subsequently incubated with a horse anti-mouse secondary antibody conjugated to fluorescein (1 : 300; Vector Laboratories Inc.) for 2 h at $22 \pm 1^\circ\text{C}$ in the dark. The secondary antibody was diluted in PBS containing 0.25% Triton X-100. Sections were washed three times for 10 min. For double-labelling of TH with SYP, PAR4 and α -syn, sections were then blocked with PBS containing 1% normal goat serum for 1 h. The slides were washed three times in PBS and then incubated overnight at 4°C with either rabbit derived anti-SYP (1 : 50), rabbit derived anti-PAR4 (1 : 250; Santa Cruz) and rabbit derived anti- α -syn (1 : 1000; Chemicon International Inc.) diluted in PBS containing 1% normal goat serum and 0.25% Triton X-100. Sections were incubated with goat anti-rabbit secondary antibody conjugated to fluorescent Cy3 (1 : 200; Chemicon International Inc.) for 1 h at $22 \pm 1^\circ\text{C}$ in the dark and its addition was preceded by three 10-min rinses in PBS. As a control, it was performed another set of experiments where the sections were only incubated with the TH antibody and then visualized with both fluorescent filters. No signal was detected when TH alone with Cy3 filter was used (photomicrograph not shown). The same was true with SYP, PAR4 and

α -syn when fluorescein filter was used. Immunofluorescence was visualized using an Olympus BX61 microscope (Tokyo, Japan). Images were acquired using a digital camera (Olympus DP70) and processed using the associated software package to the camera (Olympus DPController and Olympus DPManager).

TUNEL histochemistry

To detect DNA fragmentation *in situ*, terminal uridine nick-end labelling (TUNEL) histochemistry was performed using a modified technique of the method of Gavrieli *et al.* (1992). Animals were decapitated at different times after thrombin injection (6, 12, 24, 48 and 72 h) and the brains removed and frozen at -15°C in isopentane. Thaw-mounted 12- μm sections were post-fixed in freshly prepared 4% *p*-formaldehyde in 0.1 mol/L phosphate buffer for 10 min. Sections were then washed twice for 5 min in PBS, 5 min in 1% H_2O_2 in 100% methanol and rinsed twice for 5 min each in PBS. Sections were pre-incubated with 1x terminal transferase (TdT) buffer (Roche, Mannheim, Germany) for 10 min before being incubated for 1 h at 37°C with the following solutions per brain section: 0.75 μL TdT (Roche), 15 μL 5x TdT buffer, 0.75 μL biotin-14-dATP (Gibco, BRL, Bethesda, MD, USA) and 58.5 μL distilled water. Background and non-specific labelling was reduced by washing for 15 min at $22 \pm 1^{\circ}\text{C}$ in 2x SSC, rinsing in distilled water, incubating in 2% bovine serum albumin (BSA) in PBS for 10 min, and then in PBS for 5 min. Sections were then incubated for 1 h with the ImmunoPure[®]ABC Peroxidase staining kit diluted 1 : 100 in PBS at $22 \pm 1^{\circ}\text{C}$. Sections were developed as for immunocytochemistry, with 3,3'-diaminobenzidine as chromogen.

Double-labelling antibody and TUNEL assay

Animals were perfused and sections were prepared as described above. Section of 18- μm were cut on a cryostat and mounted in gelatin-coated slides. For double-labelling of TH with TUNEL stain, sections were rehydrated in PBS for 10 min, and then blocked with PBS containing 1% normal horse serum for 1 h. The blocking solution was replaced for rabbit derived anti-TH (1 : 1000) diluted in the blocking solution containing 0.25% Triton X-100, and the slides were then incubated overnight at 4°C . The slides were washed three times for 10 min in PBS and subsequently incubated with a horse anti-mouse secondary antibody conjugated to fluorescein (1 : 300; Vector Laboratories Inc.) for 2 h at $22 \pm 1^{\circ}\text{C}$ in the dark. The secondary antibody was diluted in PBS containing 0.25% Triton X-100. Sections were washed overnight with 1% BSA, PBS and 0.3% Triton. TUNEL-stain was performed always in the dark. Sections were incubated in 4% *p*-formaldehyde for 20 min, then washed for 30 min in PBT (0.3% Triton X-100 in PBS) and incubated in 100 mmol/L sodium citrate + 1% Triton X-100 for 30 min at 65°C . Sections were rinsed three times for 10 min each in PBT. Sections were then pre-incubated at 37°C with 1x TdT buffer (Promega, Madison, WI, USA) for 10 min before being incubated for 2 h at 37°C with the following solutions per brain section: 1.5 μL TdT (Promega), 6 μL 5x TdT buffer, 0.3 μL biotin-14-dATP (Gibco, BRL) and 22.2 μL distilled water. Background and non-specific labelling was reduced by washing for 10 min in PBT, rinsing in distilled water and washing for 15 min at $22 \pm 1^{\circ}\text{C}$ in $2 \times \text{SSC}$. Sections were rinsing in distilled water, incubating in 2% BSA in PBS for 10 min, and then in PBT for 10 min. Sections were then incubated in Fluorolink Labelled Streptavidin[®] (0.3% in PBS;

Amersham Bioscience, Little Chalfont, UK) for 30 min, rinsed twice in PBS for 10 min and mounted in glycerol: water 3 : 1. As a control, another set of experiments was performed where the sections were only incubated with TH antibody and then visualized with both fluorescence filters. No signal was detected with TH alone when Cy3 filter was used (photomicrograph not shown). The same was true with the tunnel assay when fluorescein filter was used. Immunofluorescence was visualized using an Olympus BX61 microscope. Images were acquired using a digital camera (Olympus DP70) and processed using the associated software package to the camera (Olympus DPController and Olympus DPManager).

FluoroGold

To test whether neurons were dead or simply did not express TH, 1 μL of FluoroGold (FG; Histochem, 4% in deionised water) was injected into both striata. Animals were killed after treatments and fluorescence was visualized using an Olympus BX61 microscope. Images were acquired using a digital camera (Olympus DP70) and processed using the associated software package to the camera (Olympus DPController and Olympus DPManager).

Statistical analysis

Results are typically expressed as mean \pm SD. Mean was compared by one-way ANOVA. The Fisher's least significant difference test was used for *post hoc* multiple range comparisons.

Results

Effect of the striatal injection of thrombin on substantia nigra: dopaminergic system

Injection of thrombin into the striatum induces a loss of TH-IR in the SN showed by a decrease in fibres and neuronal bodies 1 week after the injection. Although the disappearance of TH-IR is used as a marker of dopaminergic degeneration, there are some concerns about the accuracy of this marker, as the loss of TH immunostaining could also be because of loss of TH expression rather than neuronal death. Consequently, we bilaterally injected 1 μg of the retrograde tracer FG within striatum, the terminal field of the nigrostriatal projection; 1 week later, the left striatum received a single injection of 15 or 25 U of thrombin. In specimens killed 2 weeks after intra-striatal injection of thrombin (Fig. 1), TH-IR in the left SN decreased, being affected both neuronal bodies and fibres. The loss of TH-IR was accompanied by the loss of FG labelled neuronal bodies, showing that thrombin produced a retrograde degeneration of the SN and not only a down-regulation of TH expression. We have quantified the loss of dopaminergic neurons by counting the number of TH- and FG-positive bodies in the SN. TH-positive bodies decreased to a 85.0% and 79.4% of control values (11 868 \pm 587 cells) after the injection of 15 and 25 U of thrombin respectively ($p < 0.01$ in both cases); FG-positive bodies decreased to a 75.7% and 73.1% of control values (7654 \pm 774 cells) for the same doses ($p < 0.01$ in both cases).

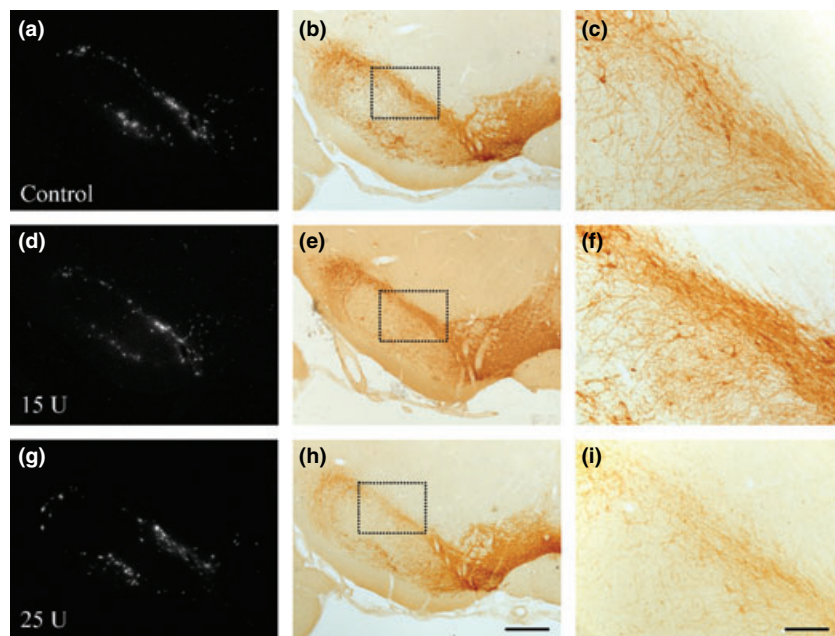


Fig. 1 Effect of the intrastratial injection of thrombin on the TH- and the FG-positive neurons in the substantia nigra. The retrograde tracer FG was injected in the left striatum 1 week prior to thrombin injection, marking neuronal cell bodies in the substantia nigra (panels a, d and g). Two weeks after thrombin injection, the left SN showed a decrease in the number of FG- and TH-positive neurons and fibres that seems to follow a dose-dependent pattern (d and e for 15 U; g and h for 25 U of thrombin respectively) compared with the untreated animal (a and b). High magnifications (c, f and i) correspond to the fields within the dotted boxes. Scale bars: (a, b, d, e, g and h) 1 mm and (c, f and i) 100 μ m.

These results were confirmed by *in situ* hybridization for TH and DAT mRNA expression (Fig. S1); there was a clearly observable decrease in TH/DAT-positive cells between -5.2 and -5.8 mm from bregma point, corresponding to plates 38–41 from the stereotaxic brain atlas of Paxinos and Watson (1986). Quantification showed a decrease in TH- and DAT-positive cells (counted together) corresponding to 68.7% of the values found in the unlesioned side, $p < 0.05$. However, GAD mRNA expression in SN did not change in these levels, suggesting that retrograde degeneration affects only the dopaminergic neuronal phenotype (Fig. S1e and f). We have also observed a topological relationship between the site of injection in the striatum and the region of TH immunonegativity in the SN. That is, a lesion in the more posterior part of the striatum led to degeneration of DA cells in the more posterior SN (not shown). This topological relationship between the striatal terminals and their parent nigral cell bodies corresponded well with the previously published tracing studies on the nigrostriatal pathway (Medina and Reiner 1995).

As a further step, we injected 25 U of thrombin within the striatum and studied its effect 2 months later using horizontal sections which allow us to observe the effect on SN and striatum in the same slice. The results shown in Fig. 2 point out that the deleterious effect produced for thrombin were not recovered 2 months after thrombin injection. Quantification at this time showed that TH-positive neurons decreased to a $78.5 \pm 7.8\%$ of control values ($p < 0.05$; Fig. 2f and g). There was also an appreciable decrease in the density of TH-positive fibres connecting SN and striatum (Fig. 2d and e), while the striatum was almost completely unaffected (Fig. 2b and c).

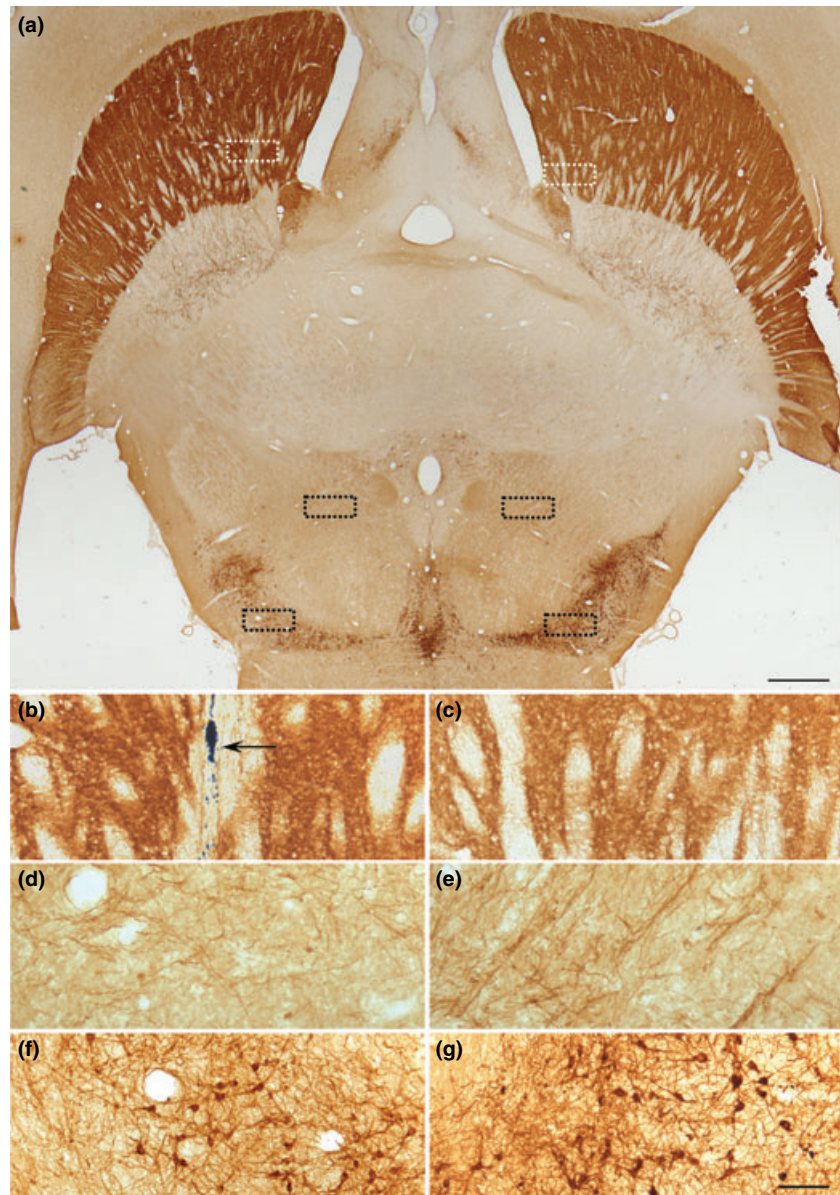
Study of the effect of thrombin injection on striatum

In the striatum, thrombin injection produced a slight loss of TH-IR restricted to a small area around the injection track. This is in agreement with a previous work, where we described the specific degeneration of dopaminergic neurons in SN by the injection of thrombin (Carreño-Müller *et al.* 2003). This is also in agreement with a report from Xue and Del Bigio (2001), showing that the injection of 25 U of thrombin in striatum causes a small area of damage. On the contrary, Fujimoto *et al.* (2007) recently showed a significant deleterious effect of intrastratial thrombin on striatal tissue. Consequently, we have carried out a careful study of the effects produced by the injection of thrombin in striatum.

We have performed immunostaining for NeuN to detect neurons as a whole and *in situ* hybridization for GAD67 mRNA expression to detect GABAergic neurons (Fig. 3). Immunohistochemistry with NeuN results in the staining of both nucleus and cytoplasm. The injection of heat-denatured thrombin produced a small loss of NeuN staining almost restricted to the needle tract (0.14 ± 0.02 mm²; Fig. 3b); the injection of 15 U of thrombin into the left striatum increased this loss, producing an area devoid of NeuN staining (0.28 ± 0.02 mm²; Fig. 3a) that was different from the control ($p < 0.01$). It is worthy to note that the size of the areas losing NeuN staining is very small; in fact, it is more than ten times smaller than the damage reported by Fujimoto *et al.* (2007).

The GABAergic system in the striatum represents the most abundant neuronal population therefore showing a high level of expression of GAD67 mRNA, an accurate index of striatal tissue preservation in response to intrastratial

Fig. 2 TH immunoreactivity 2 months after the intrastriatal injection of thrombin. Rat was injected into the left striatum with 25 U of thrombin. The right side served as control. (a) The figure shows a horizontal section of the rat brain displaying the striatum, the substantia nigra and fibres connecting both structures. Boxes mark areas of special interest within the photograph that are shown at high magnification and described below. (b and c) High magnification of the dashed boxes placed in the striatum in panel (a) showing the injection site of 25 U of thrombin (panel b; arrow shows the Monastral Blue inert tracer) and the control, untreated right side (panel c). Damage in panel (b) is closely restricted to the injection track. (d and e) High magnifications of the small black dashed boxes in panel (a), showing that TH immunopositive fibres almost disappear in the left side comparing with the untreated one. (f and g) High magnifications of the dotted boxes within the right and the left SN in panel (a). Number of TH-positive neurons and fibres decreases in the left side compared with the control side. Scale bars: (a) 500 μ m and (b–g) 50 μ m.



atal thrombin (Fig. 3c). The loss of GAD67 mRNA expression observed after heat-denatured thrombin injection into the striatum was similar in thrombin-injected animals.

As thrombin could be producing some effect on synaptic structures, we have studied its effect on two pre-synaptic boutons marker proteins, SYP and SV2. At high magnification, striatum neuropil contained many boutons immunostained for SV2 and SYP. Striatal SV2 displayed an even distribution pattern through the striatum, not affected by the injection of heat-denatured thrombin. After thrombin injection, SV2 immunoreactivity pattern was disrupted, being observed in globular, engorged structures suggesting degeneration of terminals (Fig. 4a–f). A similar result was found for SYP (Fig. 4h); in addition, we have carried out double

immunostaining for SYP (as pre-synaptic boutons marker) and TH (as dopaminergic marker); some of the 'degenerated' SYP-positive structures colocalized with TH-positive structures (Fig. 4g–i), suggesting that the degenerating terminals were dopaminergic. These results suggest that thrombin could produce the destruction/elimination of striatal dopaminergic synapses.

Effect of the striatal injection of thrombin on substantia nigra glial cells

As the degeneration process induced by thrombin also produced astrogliosis and activation of microglia (Carreño-Müller *et al.* 2003), we have studied the effect of the intrastriatal injection of thrombin on these cells in SN.

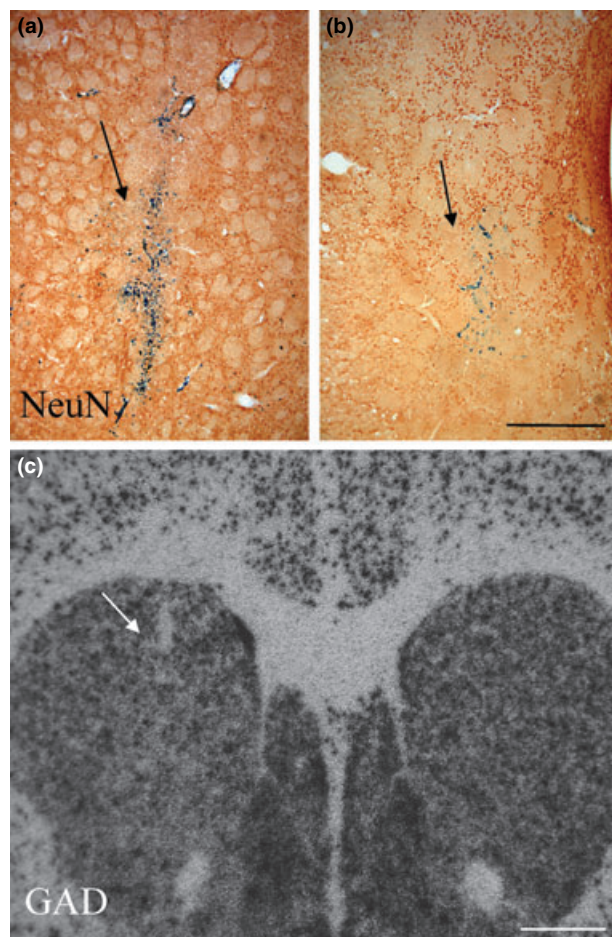


Fig. 3 Effect of thrombin injection on striatum. (a) Coronal section showing the loss of NeuN immunostaining after the injection of 15 U of thrombin. The arrow shows the injection site; the tracer is clearly visible. (b) Effect of the injection of heat-denatured thrombin; the arrow shows the injection site. (c) Photograph of a dry-film autoradiography showing a slight loss of GAD67 mRNA expression in the left striatum after the injection of 15 U of thrombin. The arrow shows the injection site of thrombin. The right side acts as control. Scale bars: (a and b) 500 μ m and (c) 1 mm.

Thrombin induced a retrograde activation of astrocytes in the ipsilateral SN (Fig. 5), as shown by GFAP immunostaining 1 week after injection. Activation affected not only the number (1153 ± 184 cells per mm^2 for left SN vs. 694 ± 68 cells per mm^2 for the right, untreated SN; $p < 0.01$) but the morphology of cells as well. Astrocytes in the left SN (Fig. 5b) appeared thicker and more intensely stained than their untreated counterparts from the right SN (Fig. 5c), with enlarged cell bodies sending hypertrophic processes to neuropil, which became covered with astrocytes forming a dense network. Two weeks after thrombin injection, astrocytes activation had reverted, showing a 'normal' appearance in both sides (not shown). However, we have not found any significant difference in the

microglial population of the SN when comparing the left and the right side neither in the number nor the morphology of cells (not shown).

Study of dopaminergic neuron death following intrastriatal injection of thrombin

In order to examine whether intrastriatal injection of thrombin induces cell death in SN, we have studied different signs of degeneration in this structure at various times after the injection of thrombin within the striatum. So, the time course showed induction of cFos in dopaminergic neurons from 6 h after thrombin injection (Fig. 6f and g). Twenty-four hours after the injection of thrombin in the striatum, we observed apoptotic nuclei in SN colocalizing with TH-positive neurons (Fig. 6a–e).

Presence of α -synuclein in substantia nigra dopaminergic neurons

Protein deposits are also a key feature of the parkinsonian brain exemplified in Lewy bodies; α -syn has been identified as the main component of Lewy bodies. In our experimental design, thrombin injection in striatum induced the appearance of α -syn inclusions; we observed this in SN dopaminergic neurons (immunostained with TH) 7 days after the injection of thrombin in striatum (Fig. 6h–j).

Role of thrombin receptors in the retrograde degenerative process induced in SN after the intrastriatal injection of thrombin

The effects observed after thrombin injection could be simply because of its unspecific proteolytic action on several proteins without intervention of PARs. To test this, we have used two short peptides with the sequence of the tethered ligands which are able to mimic thrombin activity on PAR1 and PAR4 respectively (thrombin activates PAR1, PAR3 and PAR4, but not PAR2; probably, it does not activate PAR3 neither, as it has been suggested to work mainly as a chaperone for PAR4; for review, see Coughlin 2000). So, intrastriatal administration of a PAR4 agonist peptide produced a loss of TH-positive neurons in SN (-10.3% , $p < 0.05$; Fig. 7). On the contrary, no effect was observed after the administration of a PAR1 agonist peptide (not shown). If administration of a PAR4 agonist peptide in striatum has the observed effect on SN, then PAR4 must be expressed in striatum. Thus, we have also studied the expression of PAR4 within the striatum after the injection of thrombin; although PAR4 expression showed a more or less even distribution, it seemed to be concentrated in spots which colocalize with structures that are also TH-positive (Fig. 7d–f). As no TH-positive cells exist in striatum, these TH-positive spots could be degenerating, hypertrophic dopaminergic terminals; colocalization with PAR4 expression could suggest that an over-expression of this thrombin receptor coincides with degenerating TH terminals.

Fig. 4 Effect of thrombin on the striatal TH-positive terminals. (a–c) SV2 immunoreactivity around the injection site of heat-denatured thrombin; an even reactivity can be observed. (d–f) SV2 immunoreactivity around the injection site of thrombin; engrossed immunoreactive structures can be seen. (h) SYP immunoreactivity, also showing engrossed structures that suggest terminal degeneration. Some of them colocalize with TH-positive structures (g and i). Scale bars: (a and d) 500 μ m; (b and e) 100 μ m; and (c and f–i) 50 μ m.

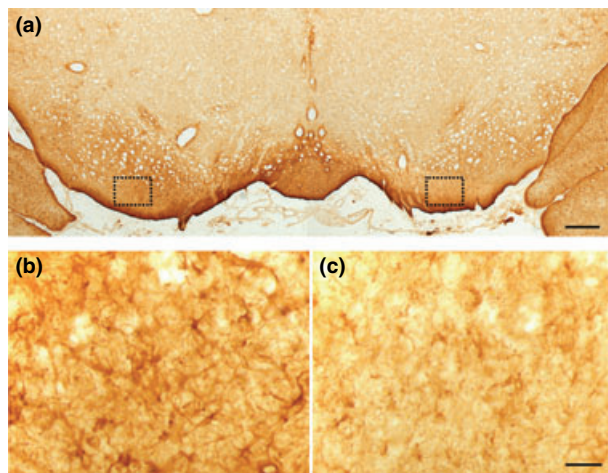
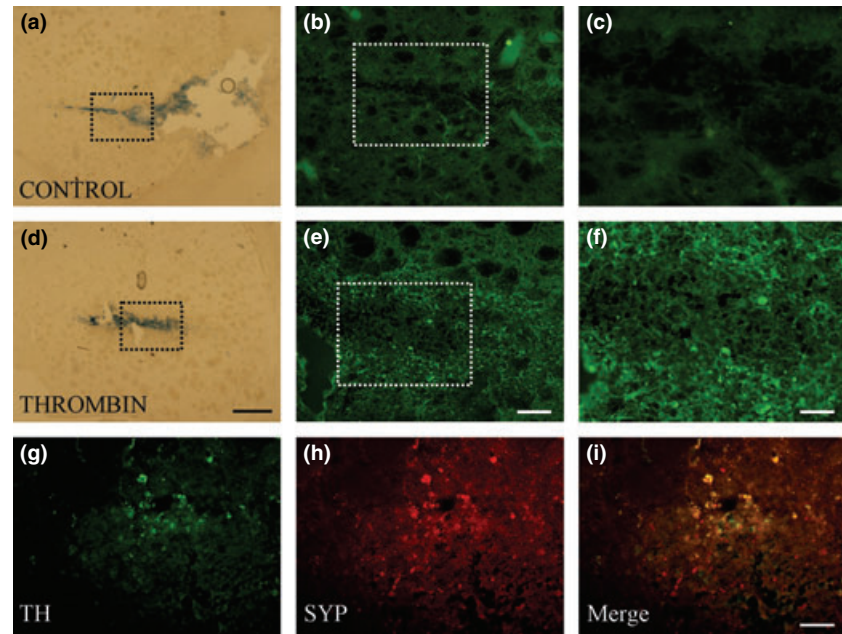


Fig. 5 Effect of the intrastratial injection of thrombin on the astroglial population in the substantia nigra. Rat was injected into the left striatum with 25 U of thrombin. The right side served as control. (a) One week after the injection, the left substantia nigra (ipsilateral to the injection) showed an increase in GFAP immunoreactivity when compared with the untreated side (right side of the panel). (b and c) High magnifications corresponding to the dashed-line boxes in panel (a). GFAP-positive structures are abundant and well defined in the left side (b); some stellate astrocytes are marked by asterisks, while arrows mark hypertrophic astrocytes. GFAP-immunoreactivity in the untreated side (c) is weaker, with some scarce stellate astrocytes (asterisks) and absence of hypertrophic astrocytes. Scale bars: (a) 500 μ m and (b and c) 50 μ m.

Discussion

In the present work, we have studied the processes by which the intrastratial injection of thrombin induced the loss of

dopaminergic neurons in SN, with preservation of the striatal tissue. The intrastratial injection of thrombin produced a loss of dopaminergic neurons projecting to the injection site as demonstrated by retrograde labelling with FG, TH-IR and TH and DAT mRNAs expression. However, there were no changes in GAD mRNA in SN pars reticulata. Nigral dopaminergic cells loss was only significant in the SN ipsilateral to the injection; after the injection of thrombin, most of TH-IR neurons in the ipsilateral side displayed shrunken and round-shaped cell bodies with few processes compared with the control side. Neurodegeneration was accompanied by astrogliosis seen as increase in GFAP-positive structures in the ipsilateral SN.

In contrast, thrombin injection produced a slight loss of TH-IR in the striatum restricted to a small area around the injection track, in agreement with a previous report (Carreño-Müller *et al.* 2003). Additional immunostaining (NeuN) was performed for the unspecific detection of neurons; *in situ* hybridization for GAD67 mRNA expression allowed us to detect GABAergic neurons specifically. We only found a slight loss of neurons. Our results, however, contrast with those of Fujimoto *et al.* (2007) but fully agree with those of Xue and Del Bigio (2001). Fujimoto *et al.* (2007) injected a single intrastratial dose of 20 U thrombin, inducing a massive region of striatal neurotoxicity as large as 3.44 mm² in terms of NeuN immunoreactivity. This effect is reminiscent of a potent metabolic poisoning, like that produced by 3-nitropropionic acid (Beal *et al.* 1993), malonate (Zeevalk *et al.* 2000) or rotenone (Ferrante *et al.* 1997). In contrast to this effect, our study demonstrates a limited damage close to the injection tract, in accordance with the study by Xue and Del Bigio (2001). In some animals, we have observed large lesions in terms of NeuN

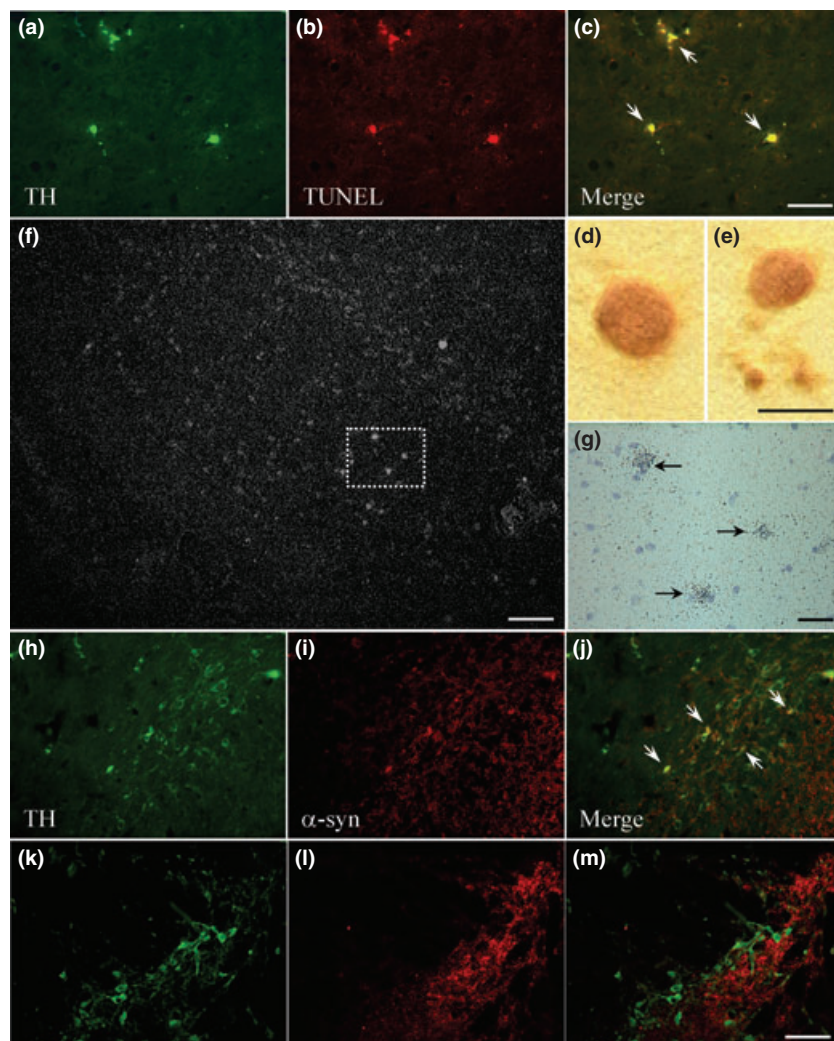


Fig. 6 Features of neuronal degeneration in SN after the intrastriatal injection of thrombin. TH-positive neurons in the SN (a) colocalizing with apoptotic nucleus (b and c). A high magnification of apoptotic nucleus is shown (d and e). The dark-field photography (f) shows some cFos-positive nucleus in the SN. A bright-field magnification is shown (g). Inclusions of α -syn can be observed in SN (i) after the injection of thrombin in striatum. Some of them (arrows in panel j) colocalize with TH-positive structures (h and j). The injection of heat-denatured thrombin in striatum did not produce colocalization of TH and α -syn (k–m). Scale bars: (a–c and h–m) 50 μ m; (d and e) 5 μ m; (f) 500 μ m; and (g) 25 μ m.

immunoreactivity which were unequivocally related to blood extravasations from the vascular compartment to the brain parenchyma and hence discarded from our study.

Retrograde destruction of DA cell bodies in the SN has been described previously in adult animals, mostly related to energy impairment at their terminal projection site (Sonsalla *et al.* 1997) by 6-hydroxydopamine (Marti *et al.* 2002), MPP⁺ (Miwa *et al.* 2004), 3-nitropropionic acid (Waldner *et al.* 2001) and malonate (Sonsalla *et al.* 1997), or alternatively after axotomy of the medial forebrain bundle (Venero *et al.* 1997). These neurotoxins induce large striatal lesions along with a strong energy dysfunction, which is a well documented cause of dopaminergic neurons death (Sonsalla *et al.* 1997). It is interesting to note that striatal ischaemic lesions induced a transient down-regulation of TH synthesis without reduction in the number of SNc TH neurons (Soriano *et al.* 1997) that was prevented by administration of GABA agonist (Yamada *et al.* 1996). Moreover, the striatal injury induced in adult animals by excitotoxins as ibotenic or

quinolinic acid produced a degeneration of GABAergic neurons in SN pars reticulata, while there was no degeneration or loss of dopaminergic neurons within SNc (DeGiorgio *et al.* 1998). On the contrary, these injuries produced some kind of protection to the dopaminergic system against different insults as MPP⁺, 6-hydroxydopamine or methamphetamine (O'Dell *et al.* 1994; Venero *et al.* 1995; Matarredona *et al.* 2001). The axon-sparing injury of the striatum during development, either because of hypoxia-ischaemia or intrastriatal injection of an excitotoxin, resulted in a decrease in the number of dopaminergic neurons in the adult SN as consequence of DA neuron death (Burke *et al.* 1992). In this model, neuronal death is produced by apoptosis, identified within phenotypically defined DA neurons (Macaya *et al.* 1994).

As a further step, we have studied the degenerative process that produces the loss of dopaminergic neurons. After striatal thrombin injection, cFos mRNA expression was up-regulated in SN neurons ipsilateral to the injection site. In contrast, no

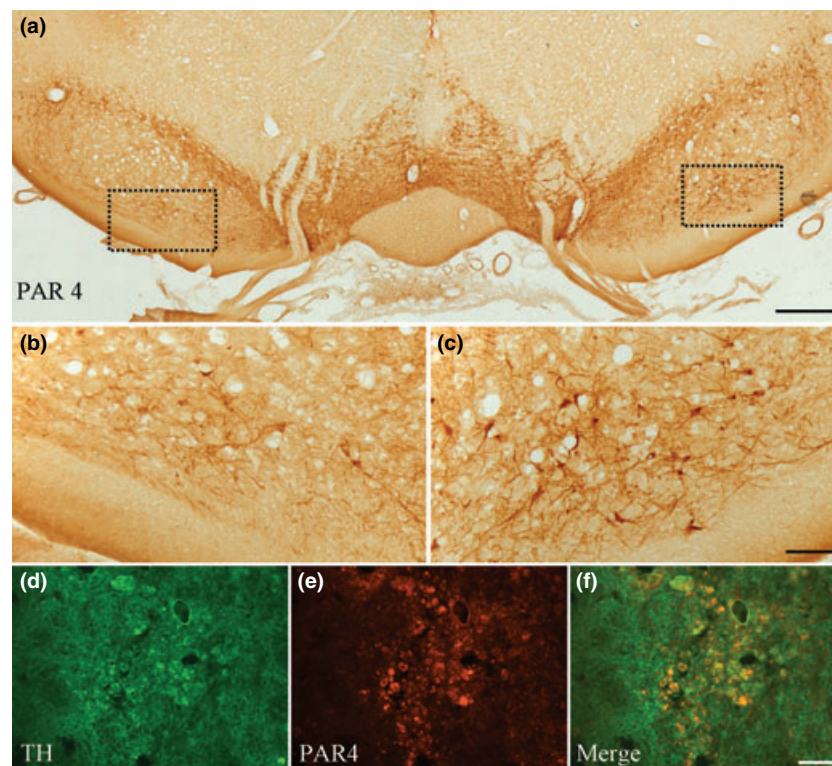


Fig. 7 Involvement of PAR4 receptor in the retrograde nigral degeneration induced by the striatal injection of thrombin. (a) Injection of the PAR agonist peptide GYPGKF into the left striatum induced a loss of TH-positive structures in the ipsilateral SN. (b) High magnification of the field in the dotted box in the left side of panel (a). (c) High magnification of the field in the dotted box in the right side of panel (a), showing TH immunohistochemistry in a control. (e) Photograph from striatum showing positive immunoreactivity to an anti-PAR4 antibody: These structures also show TH immunoreactivity (d and f). Scale bars: (a) 500 μm ; (b and c) 100 μm ; (d–f) 50 μm .

cFos mRNA expression was detected in the non-injected side. The induction of immediate early genes suggests ipsilateral transynaptic modulation of neuronal activity. Further, we also found cells with apoptotic bodies. In addition, we observed accumulation of α -syn in dopaminergic neurons of the SNc 7 days after injection, suggesting that thrombin injection in the striatum can induce protein mishandling in SNc. These TUNEL- and α -syn-positive cells colocalized with TH in the SN ipsilateral to the injection. These results suggest that injection of thrombin into striatum produced accumulation of α -syn and retrograde degeneration of SN dopaminergic neurons that die by apoptosis.

Next, we studied the involvement of PARs in the effect of thrombin using two short peptides which are agonists for PAR1 and PAR4 respectively. Our results showed that the agonist peptide for PAR4 but not for PAR1 produced an effect similar to thrombin. Therefore, we suggest that under our experimental conditions thrombin might trigger dopaminergic neurons degeneration via PAR4, which could be involved in thrombin-induced neurotoxicity (Wang *et al.* 2002). Moreover, Choi *et al.* (2003b) reported that the PAR4-activating peptide GYPGKF caused death of dopaminergic neurons in mesencephalic cultures. These findings call attention for the potential pathogenic roles of PAR4 signalling in cerebrovascular damage-associated neurodegenerative disorders and highlights potential therapeutic values of reagents that can inhibit PAR4 signalling or the

persistent p44/42 mitogen-activated protein kinase activation in these diseases. PARs mRNAs express in neurons and astrocytes (Weinstein *et al.* 1995) and there is evidence of functional receptors in both cell types (Wang *et al.* 2002). We also show that PAR4 colocalizes with TH in striatum. The axonal injury induced for thrombin seems to be produced through $[\text{Ca}^{2+}]_i$ overload (Stys 2004). This could be because of the inhibition of adenylate cyclase and the activation of phospholipase C, stimulating IP_3 formation with the consequent increase in $[\text{Ca}^{2+}]_i$ released from internal stores (Hung *et al.* 1992).

In an effort to find a rationale for the loss dopaminergic neurons in response to the intra-striatal injection of thrombin, we found an increase in SYP immunoreactivity (a component of synaptic vesicles in pre-synaptic terminals) within striatal TH terminals; SYP immunoreactivity followed a granular pattern, indicating accumulation of synaptic vesicles in pre-synaptic terminals, which is associated to degenerative processes. Similar results were found for SV2, another component of synaptic vesicles. Increase in SYP and SV2 immunoreactivity in the striatum following local thrombin injection reflects inhibition of synaptic vesicle transport and dysfunction of synapse, thus providing a histological substrate for brain dysfunctions. Moreover, SYP seems to be involved in pre-synaptic functions such as vesicle-membrane fusion and release of neurotransmitters, which induces a transient increase in the pre-synaptic functions followed by a decrease in functional pre-synaptic activity, the

loss of post-synaptic response and consequently the trans-synaptic retrograde degeneration of axon terminals. All these data suggest that thrombin is able to induce retrograde degeneration of the dopaminergic system from striatum, maybe triggering the activation of PAR4 along with the destruction of pre-synaptic elements with the consequent synapse elimination.

Neuronal loss produced by synapse elimination has been shown and studied especially in muscle junction during the perinatal period; it is interesting to note that thrombin seems to be involved in this process, although its precise molecular mechanism is not known (Zoubine *et al.* 1996). Two different mechanisms have been suggested: competition between terminals, based on dwindling supplies of essential neurotrophic factors; and imbalanced, excess local protease activity (Vrbova and Fisher 1989). Moreover, thrombin is required for activity-dependent synapse elimination *in vitro* (Liu *et al.* 1994) and *in vivo* (Zoubine *et al.* 1996). Local injection of hirudin, an inhibitor of thrombin, retarded synapse elimination (Lanuza *et al.* 2001).

Our results could be justified according to the effect described for thrombin on motor neurons, in which it activates intracellular protease pathways inducing apoptosis through activation of its receptors (Smirnova *et al.* 2001). Presence of thrombin could be the result of intracerebral haemorrhage (ICH); prothrombin circulates in blood at concentrations within the micromolar range (Lee *et al.* 1995) and is readily converted into thrombin after vascular injury. Spontaneous ICH is a devastating type of stroke accounting for approximately 8–14% of all strokes in western countries. Interestingly, ICH occurs preferentially in cerebral cortex and striatum (Fujimoto *et al.* 2007). Imamura *et al.* (2003) have recently shown neurodegeneration and atrophy in the ipsilateral SN using a collagenase-induced model of ICH within the striatum. Thrombin could be one of the factors responsible for the damage shown by these authors. This establishes a relationship between the nigral dopaminergic neuronal degeneration characterizing PD and the occurrence of physical trauma and ICH in distant areas such as striatum. Occurrence of apoptosis in this process could be in agreement with the evidence of nigral cell apoptosis in PD shown in some clinical studies. Prothrombin mRNA is expressed by cells of the nervous system (Dihanich *et al.* 1991); significant amounts of thrombin can be generated by this mechanism and persist where cerebrovascular damage occurs. Such high concentrations of thrombin cause brain damage (Lee *et al.* 1995) and could also contribute to damage in degenerative processes such as Alzheimer's disease and vascular dementia (Grammas *et al.* 2004). At the same time, little is known about the effect of aging on synapses in the mammalian nervous system. Coggan *et al.* (2004) demonstrated primary, age-associated synapse elimination with functional consequences in mouse submandib-

ular ganglion neurons. This rise the question whether synapse elimination could be involved in some neurodegenerative processes and which could be the molecular mechanism.

Acknowledgements

This work was supported by Grants SAF2004-06601 and SAF2005-02847. RMdP thanks the Junta de Andalucía for a Contrato within the framework of Grupos de Excelencia. RFV thanks the Spanish Ministerio de Educación y Ciencia for a FPI fellowship. We thank Mr J. P. Calero for his skilful technical assistance.

Supplementary material

The following supplementary material is available for this article online:

Fig. S1 TH, DAT and GAD mRNA *in situ* hybridization in SN after the intrastratial injection of thrombin.

This material is available as part of the online article from <http://www.blackwell-synergy.com>.

Please note: Blackwell Publishing are not responsible for the content or functionality of any supplementary materials supplied by the authors. Any queries (other than missing material) should be directed to the corresponding author for the article.

References

- Beal M. F., Brouillet E., Jenkins B. G., Ferrante R. J., Kowall N. W., Miller J. M., Storey E., Srivastava R., Rosen B. R. and Hyman B. T. (1993) Neurochemical and histologic characterization of striatal excitotoxic lesions produced by the mitochondrial toxin 3-nitropropionic acid. *Neurosci.* **13**, 4181–4192.
- Beecher K. L., Andersen T. T., Fenton J. W. 2nd and Festoff B. W. (1994) Thrombin receptor peptides induce shape change in neonatal murine astrocytes in culture. *J. Neurosci. Res.* **37**, 108–115.
- Burke R. E., Macaya A., DeVivo D., Kenyon N. and Janec E. M. (1992) Neonatal hypoxic-ischemic or excitotoxic striatal injury results in a decreased adult number of substantia nigra neurons. *Neuroscience* **50**, 559–569.
- Carreño-Müller E., Herrera A. J., dePablos R. M., Tomás-Camardiel M., Venero J. L., Cano J. and Machado A. (2003) Thrombin induces *in vivo* degeneration of nigral dopaminergic neurones along with the activation of microglia. *J. Neurochem.* **84**, 1201–1214.
- Chartier-Harlin M. C., Kachergus J., Roumier C. *et al.* (2004) Alpha-synuclein locus duplication as a cause of familial Parkinson's disease. *Lancet* **364**, 1167–1169.
- Choi S. H., Joe E. H., Kim S. U. and Jin B. K. (2003a) Thrombin-induced microglial activation produces degeneration of nigral dopaminergic neurons *in vivo*. *J. Neurosci.* **23**, 5877–5886.
- Choi S. H., Lee D. Y., Ryu J. K., Kim J., Joe E. H. and Jin B. K. (2003b) Thrombin induces nigral dopaminergic neurodegeneration *in vivo* by altering expression of death-related proteins. *Neurobiol. Dis.* **14**, 181–193.
- Coggan J. S., Grutzendler J., Bishop D. L., Cook M. R., Gan W., Heym J. and Lichtman J. W. (2004) Age-associated synapse elimination in mouse parasympathetic ganglia. *J. Neurobiol.* **60**, 214–226.
- Coughlin S. R. (2000) Thrombin signalling and protease-activated receptors. *Nature* **407**, 258–264.

- DeGiorgio L. A., Dibinis C., Milner T. A., Saji M. and Volpe B. T. (1998) Histological and temporal characteristics of nigral trans-neuronal degeneration after striatal injury. *Brain Res.* **795**, 1–9.
- Dihanich M., Kaser M., Reinhard E., Cunningham D. and Monard D. (1991) Prothrombin mRNA is expressed by cells of the nervous system. *Neuron* **6**, 575–581.
- Erlander M. G., Tillakaratne N. J., Feldblum S., Patel N. and Tobin A. J. (1991) Two genes encode distinct glutamate decarboxylases. *Neuron* **7**, 91–100.
- Farrer M., Gwinn-Hardy K., Muentner M. *et al.* (1999) A chromosome 4p haplotype segregating with Parkinson's disease and postural tremor. *Hum. Mol. Genet.* **8**, 81–85.
- Ferrante R. J., Schulz J. B., Kowall N. W. and Beal M. F. (1997) Systemic administration of rotenone produces selective damage in the striatum and globus pallidus, but not in the substantia nigra. *Brain Res.* **753**, 157–162.
- Fujimoto S., Katsuki H., Ohnishi M., Takagi M., Kume T. and Akaike A. (2007) Thrombin induces striatal neurotoxicity depending on mitogen-activated protein kinase pathways in vivo. *Neuroscience* **144**, 694–701.
- Gavrieli Y., Sherman Y. and Ben-Sasson S. A. (1992) Identification of programmed cell death in situ via specific labelling of nuclear DNA fragmentation. *J. Cell Biol.* **119**, 493–501.
- Grammas P., Ottman T., Reimann-Philipp U., Larabee J. and Weigel P. H. (2004) Injured brain endothelial cells release neurotoxic thrombin. *J. Alzheimers Dis.* **6**, 275–281.
- Gundersen H. G. J., Bagger P., Bendtsen T. F. *et al.* (1988) The new stereological tools: dissector, fractionator, nucleator, and point sampled intercepts and their use in pathological research and diagnosis. *Acta Pathol. Microbiol. Immunol. Scand.* **96**, 857–881.
- Hung D. T., Wong Y. H., Vu T. K. and Coughlin S. R. (1992) The cloned platelet thrombin receptor couples to at least two distinct effectors to stimulate phosphoinositide hydrolysis and inhibit adenylyl cyclase. *J. Biol. Chem.* **267**, 20831–20834.
- Imamura N., Hida H., Aihara N., Ishida K., Kanda Y., Nishino H. and Yamada K. (2003) Neurodegeneration of substantia nigra accompanied with macrophage/microglia infiltration after intrastriatal hemorrhage. *Neurosci. Res.* **46**, 289–298.
- Kruger R., Kuhn W., Muller T., Voitalla D., Graeber M., Kosel S., Przuntek H., Epplen J. T., Schols L. and Riess O. (1998) Ala30Pro mutation in the gene encoding alpha-synuclein in Parkinson's disease. *Nat. Genet.* **18**, 106–108.
- Lanuza M. A., Garcia N., Santafe M., Nelson P. G., Fenoll-Brunet M. R. and Tomas J. (2001) Pertussis toxin-sensitive G-protein and protein kinase C activity are involved in normal synapse elimination in the neonatal rat muscle. *J. Neurosci. Res.* **63**, 330–340.
- Lee K. R., Betz A. L., Keep R. F., Chenevert T. L., Kim S. and Hoff J. T. (1995) Intracerebral infusion of thrombin as a cause of brain edema. *J. Neurosurg.* **83**, 1045–1050.
- Liu Y., Fields R. D., Festoff B. W. and Nelson P. G. (1994) Proteolytic action of thrombin is required for electrical activity-dependent synapse reduction. *Proc. Natl Acad. Sci. USA* **91**, 10300–10304.
- Macaya A., Munell F., Gubits R. M. and Burke R. E. (1994) Apoptosis in substantia nigra following developmental striatal excitotoxic injury. *Proc. Natl Acad. Sci. USA* **91**, 8117–8121.
- Marti M. J., Saura J., Burke R. E., Jackson-Lewis V., Jimenez A., Bonastre M. and Tolosa E. (2002) Striatal 6-hydroxydopamine induces apoptosis of nigral neurons in the adult rat. *Brain Res.* **958**, 185–191.
- Matarredona E. R., Santiago M., Venero J. L., Cano J. and Machado A. (2001) Group II metabotropic glutamate receptor activation protects striatal dopaminergic nerve terminals against MPP⁺-induced neurotoxicity along with brain-derived neurotrophic factor induction. *J. Neurochem.* **76**, 351–360.
- Medina L. and Reiner A. (1995) Neurotransmitter organization and connectivity of the basal ganglia in vertebrates: implications for the evolution of basal ganglia. *Brain Behav. Evol.* **46**, 235–258.
- Miwa H., Kubo T., Morita S., Nakanishi I. and Kondo T. (2004) Oxidative stress and microglial activation in substantia nigra following striatal MPP⁺. *Neuroreport* **15**, 1039–1044.
- Noorbakhsh F., Vergnolle N., Hollenberg M. D. and Power C. (2003) Proteinase-activated receptors in the nervous system. *Nat. Rev. Neurosci.* **4**, 981–990.
- O'Dell S. J., Weihmuller F. B., McPherson R. J. and Marshall J. F. (1994) Excitotoxic striatal lesions protect against subsequent methamphetamine-induced dopamine depletions. *J. Pharmacol. Exp. Ther.* **269**, 1319–1325.
- Paxinos G. and Watson C. (1986) *The rat Brain in Stereotaxic Coordinates*. Academic Press, San Diego.
- Sauer H. and Oertel W. H. (1994) Progressive degeneration of nigrostriatal dopamine neurons following intrastriatal terminal lesions with 6-hydroxydopamine: a combined retrograde tracing and immunocytochemical study in the rat. *Neuroscience* **59**, 401–415.
- Smirnova I. V., Citron B. A., Arnold P. M. and Festoff B. W. (2001) Neuroprotective signal transduction in model motor neurons exposed to thrombin: G-protein modulation effects on neurite outgrowth Ca²⁺ mobilization and apoptosis. *J. Neurobiol.* **48**, 87–100.
- Smith-Swintosky V. L., Zimmer S., Fenton J. W. 2nd and Mattson M. P. (1995) Protease nexin-1 and thrombin modulate neuronal Ca²⁺ homeostasis and sensitivity to glucose deprivation-induced injury. *J. Neurosci.* **5**, 5840–5850.
- Sonsalla P. K., Manzino L., Sinton C. M., Liang C. L., German D. C. and Zeevalk G. D. (1997) Inhibition of striatal energy metabolism produces cell loss in the ipsilateral substantia nigra. *Brain Res.* **773**, 223–226.
- Soriano M. A., Justicia C., Ferrer I., Rodríguez-Farre E. and Planas A. M. (1997) Striatal infarction in the rat causes a transient reduction of tyrosine hydroxylase immunoreactivity in the ipsilateral substantia nigra. *Neurobiol. Dis.* **4**, 376–385.
- Striggow F., Riek-Burchardt M., Kiesel A., Schmidt W., Henrich-Noack P., Breder J., Krug M., Reyman K. G. and Reiser G. (2001) Four different types of protease-activated receptors are widely expressed in the brain and are up-regulated in hippocampus by severe ischemia. *Eur. J. Neurosci.* **14**, 595–608.
- Stys P. K. (2004) White matter injury mechanisms. *Curr. Mol. Med.* **4**, 113–130.
- Venero J. L., Romero-Ramos M., Revuelta M., Machado A. and Cano J. (1995) Intrastriatal quinolinic acid injections protect against 6-hydroxydopamine-induced lesions of the dopaminergic nigrostriatal system. *Brain Res.* **672**, 153–158.
- Venero J. L., Revuelta M., Cano J. and Machado A. (1997) Time course changes in the dopaminergic nigrostriatal system following transection of the medial forebrain bundle: detection of oxidatively modified proteins in substantia nigra. *J. Neurochem.* **68**, 2458–2468.
- Vrbova G. and Fisher T. J. (1989) The effect of inhibiting the calcium activated neutral protease on motor unit size after partial denervation of the rat soleus muscle. *Eur. J. Neurosci.* **1**, 616–625.
- Waldner R., Puschban Z., Scherfler C., Seppi K., Jellinger K., Poewe W. and Wenning G. K. (2001) No functional effects of embryonic neuronal grafts on motor deficits in a 3-nitropropionic acid rat model of advanced striatonigral degeneration (multiple system atrophy). *Neuroscience* **102**, 581–592.
- Wang H., Uhl J. J., Stricker R. and Reiser G. (2002) Thrombin (PAR-1)-induced proliferation in astrocytes via MAPK involves multiple

- signalling pathways. *Am. J. Physiol. Cell Physiol.* **283**, C1351–C1364.
- Weinstein J. R., Gold S. J., Cunningham D. D. and Gall C. M. (1995) Cellular localization of thrombin receptor mRNA in rat brain: expression by mesencephalic dopaminergic neurons and codistribution with prothrombin mRNA. *J. Neurosci.* **15**, 2906–2919.
- Xue M. and Del Bigio M. R. (2001) Acute tissue damage after injections of thrombin and plasmin into rat striatum. *Stroke* **32**, 2164–2169.
- Yamada K., Goto S., Yoshikawa M. and Ushio Y. (1996) Gabaergic transmission and tyrosine hydroxylase expression in the nigral dopaminergic neurons: an in vivo study using a reversible ischemia model of rats. *Neuroscience* **73**, 783–789.
- Yang Y., Akiyama H., Fenton J. W. 2nd and Brewer G. J. (1997) Thrombin receptor on rat primary hippocampal neurons: coupled calcium and cAMP responses. *Brain Res.* **761**, 11–18.
- Zeevalk G. D., Manzino L. and Sonsalla P. K. (2000) NMDA receptors modulate dopamine loss due to energy impairment in the substantia nigra but not striatum. *Exp. Neurol.* **161**, 638–646.
- Zoubine M. N., Ma J. Y., Smirnova I. V., Citron B. A. and Festoff B. W. (1996) A molecular mechanism for synapse elimination: novel inhibition of locally generated thrombin delays synapse loss in neonatal mouse muscle. *Dev. Biol.* **179**, 447–457.